Kinetics of the Aluminum-Chlorine Reaction

CHARLES COZEWITH and KUN LI

Carnegie Institute of Technology, Pittsburgh, Pennsylvania

The reaction between aluminum, in the form of flat plates, and chlorine was investigated in a flow system at temperatures from 500° to 650°F. Gaseous aluminum chloride was the reaction product at these temperatures. At 500°F. the reaction proceeded by pitting, and the rate appeared to be chemically controlled. The reaction mechanism changed at higher temperatures to give a smooth reacted surface, and the reaction rate was found to be dependent upon both mass transport and kinetic parameters. The method proposed by Rosner for calculating mass transport-dependent reaction rates was found to correlate both average and local rate data and was used to obtain estimates of the kinetic parameters for the heterogeneous surface reaction.

The reaction between aluminum and chlorine has been investigated only briefly in the past (2, 5), and no accurate reaction rate data were obtained. Consequently, this study was initiated to investigate the factors which influence the reaction rate. Within the temperature limits of this investigation, the reaction proceeds according to the equation

$$2\,Al(s) + 3\,Cl_2(g) \rightarrow Al_2Cl_6(g)$$

Experiments were carried out in a system with chlorine flowing past a flat plate of aluminum. The flow rates of chlorine were such that a laminar boundary layer was maintained over the length of the reacting surface.

EXPERIMENTAL METHODS

Apparatus and Procedure

A simplified flow diagram of the experimental apparatus is shown in Figure 1. The reactor consisted of a 3-ft. long 2-in. I.D. stainless steel tube which was electrically heated. The front 2 ft. of the reactor were packed and served as a gas preheater, while the rear section contained the aluminum plates.

The aluminum plates measured 2½ in. by 9/16 in. by 0.060 in. and rested on a hollow stainless steel plate measuring 2½ in. by ⅝ in. by ⅛ in. with a sharp leading edge. Oil was circulated through the stainless steel plate during a run to remove the heat of reaction.

Two thermocouples, contained in sheaths 0.020 in. O.D., passed into the reactor and rested on the plate surface ½ in. from the leading and trailing edges. The leading edge thermocouple was connected to a recorder-controller which operated a control valve on the inlet coolant line to the cooling plate. By this means constant surface temperatures were maintained during a run, and local temperature variations did not exceed ± 5°F.

Chlorine and nitrogen gas manifolds were connected to the inlet of the reactor. Dry nitrogen was flowed through the system before and after a run for preheating and then for cooling. Gas flow rates were measured with rotameters.

The chlorine and aluminum chloride exiting from the reactor during a run passed first into a stirred, water filled absorber for aluminum chloride absorption, and then the remaining chlorine gas entered a packed column and was absorbed in sodium hydroxide solution.

The experimental procedure consisted of placing a weighed aluminum specimen of known surface area in the reactor and then heating the system to the desired temperature in a stream of dry nitrogen. When steady state was obtained, the nitrogen flow was shut off and the chlorine flow begun. At the end of a run the chlorine flow was shut off and the nitrogen flow restarted to remove chlorine from the system. The reacted aluminum sample was then removed and weighed and the surface area measured. No reaction occurred on the bottom of the sample which was in contact with the cooling plate.

The length of a run varied from 1.5 to 7 min., and the system was assumed to be at steady state during this time. This assumption was checked by making several runs under identical conditions except for varying reaction time. The agreement between the results of duplicate runs was good.

Specimen Preparation

In order for the reaction rate data to be of use the aluminum surface activity must be uniform, that is, the aluminum must react smoothly, without pitting, so that unaccountable surface area changes do not occur during reaction. Initial exploratory work with various aluminum alloys showed that the surface activity depended upon the alloy composition, grain size, and initial surface preparation.

The best results were obtained with fully annealed 1,100 aluminum alloy, containing 99.3% aluminum, and with about 1,000 grains/sq. mm. Active surfaces were obtained by electropolishing the samples to get a smooth, clean surface and then removing the surface oxide immediately prior to reaction by immersing the samples for 1 min. at 190°F. in an acid solution containing 940 ml. of 85% H_3PO_4, 50 ml. of 70% HNO_3, 10 ml. of H_2O, and 0.3 g. of $Cu(NO_3)_2$ 3 H_2O. Samples of 1,100 alloy prepared in this manner gave smooth reacted surfaces at temperatures above 500°F. but pitted at lower temperatures.

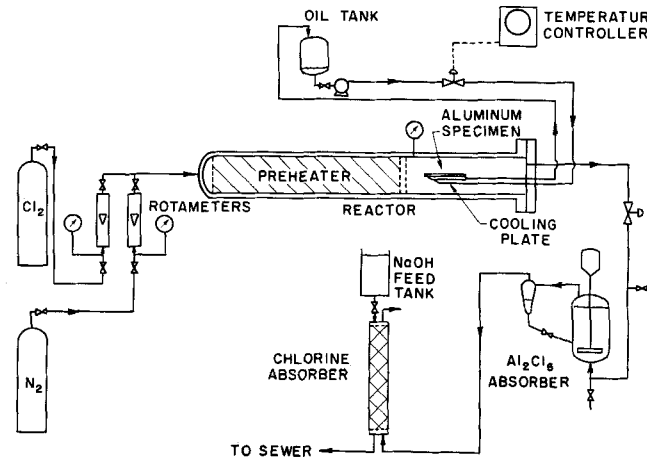

Fig. 1. Experimental apparatus.

Charles Cozewith is with Esso Research and Engineering Company, Linden, New Jersey.

Calculation of Reaction Rates

The basic equation used for reaction rate calculations was

$$R_{Al} = -\frac{dw}{A d\theta} \qquad (1)$$

where $dW/d\theta$ is the rate of weight loss of the aluminum specimen and A is the plate area.

Over the duration of any given run, the plate area was not constant owing primarily to a changing thickness from front to back and a changing length of the plate. Only slight changes in width occurred. Through a relationship between the plate area and weight, Equation (1) was integrated to give the average reaction rate based on the total plate area as

$$\bar{R}_{Al} = \frac{(W^i - W^f)}{(\theta^i - \theta^f)} \frac{(\ln A^i/A^f)}{(A^i - A^f)} \qquad (2)$$

where superscripts i and f indicate the initial and final conditions.

Data for local rate calculation were obtained by sectioning reacted specimens into ¼-in. long pieces and weighing and measuring each piece. The local reaction rate was then calculated by using Equation (2) for each ¼-in. long piece.

RESULTS AND DISCUSSION

Data were obtained at 505°, 558°, 604°, and 651°F. with chlorine flows of about 0.049 to 0.200 lb./min. as shown in Table 1. Flow in the reactor was laminar at these flow rates. The upper limits of flow and temperature were set by apparatus limitations. The pressure was 1.1 atm. for most runs, but at 604°F. pressure up to 2.2 atm. were investigated.

At 558°, 604°, and 651°F. the reacted sample surfaces were smooth, and the reaction rate could be readily determined since the surface area could be calculated. At each of these temperatures several runs were made at constant flow rate but with varying reaction time. The reaction rates determined from these runs showed good agreement, indicating both steady state and reproducible initial surface activity for the aluminum specimens.

At 505°F. the reacted aluminum surfaces were pitted, and the data obtained at this temperature are of limited utility since the true sample surface area is not known.

Table 1. Typical Average Rate Data*

Temperature, °F.	Cl_2 pressure, atm.	Cl_2 flow rate, lb./min.	Al reaction rate × 10^4, lb./(min.)(sq. in.)
500	1.22	0.0500	2.41
505	1.20	0.131	2.57
508	1.16	0.0758	2.08
555	1.10	0.113	3.15
555	1.18	0.161	3.76
560	1.17	0.114	3.07
595	1.15	0.0484	2.84
600	1.20	0.104	3.68
605	1.21	0.0769	3.39
605	1.29	0.200	4.03
608	2.17	0.137	4.72
647	1.18	0.0768	3.64
649	1.30	0.193	4.67
650	1.21	0.161	4.45
655	1.18	0.131	4.05

* Complete tabular material has been deposited as document 9452 with the American Documentation Institute, Photoduplication Service, Library of Congress, Washington 25, D. C., and may be obtained for $1.25 for photoprints or 35-mm. microfilm.

Average Rate Data

Since both the rate of reaction at the plate surface and counterdiffusion of chlorine and aluminum chloride to and from the surface can influence the measured reaction rates, the average rate data were first tested to determine the extent of transport control.

Several authors (*8* to *10*, *12*) by solution of the diffusion and momentum equations for a laminar boundary layer have obtained equations applicable to calculation of transport-controlled reaction rates for gas-solid reactions of the type

$$aA(g) + bB(s) \rightleftharpoons cC(g) \qquad (3)$$

The solution by Merk (*8*) is particularly suitable for calculation and gives the average mass flux of reactant A, equal to the average reaction rate, as

$$\bar{n}_A = \frac{\rho_s B D_A}{(1+\alpha) L} \bar{N}_{Sh} \qquad (4)$$

where

$$B = \frac{(1+\alpha)}{1 - \omega_{A,s}(1+\alpha)} (\omega_{A,s} - \omega_{A,e}) \qquad (5)$$

$$\alpha = -\frac{c M_C}{a M_A} \qquad (6)$$

$$\bar{N}_{Sh} = \sqrt{2}\, E_o\, x_D \sqrt{N_{Re}} \qquad (7)$$

The parameter E_o is a function of the Schmidt number, while x_D depends upon both the Schmidt number and B. If the surface reaction is irreversible as it is for the aluminum–chlorine reaction, then for transport control, $\omega_{A,s}$ equals zero and Equation (5) reduces to

$$B_o = -(1+\alpha)\, \omega_{A,e} \qquad (8)$$

It is also noted that the mass fluxes of A and B are related by

$$\bar{n}_B = (1+\alpha)\, \bar{n}_A \qquad (9)$$

If the aluminum–chlorine reaction is transport controlled, Equation (4) suggests that a logarithmic plot of $\bar{R}_{Al}\, L/B_o$ vs. $G\, L$ at constant temperature should be linear

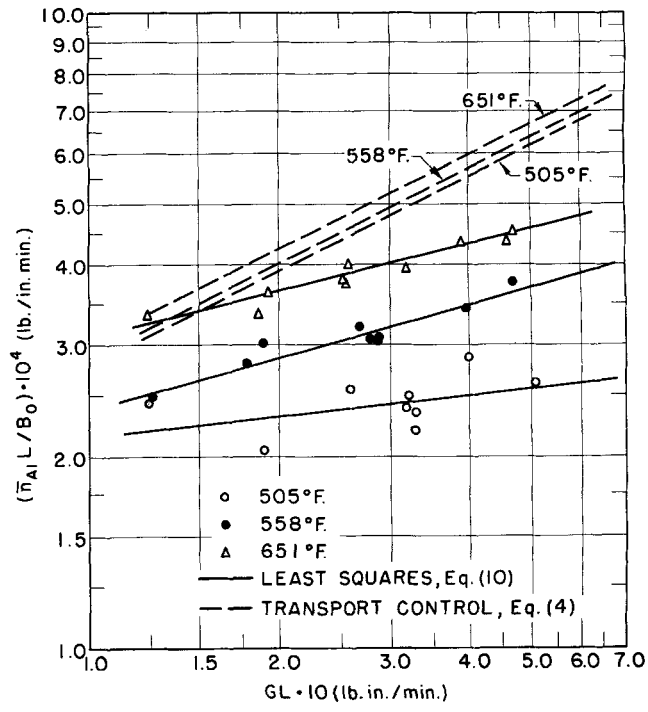

Fig. 2. Average rate data at 505°, 558°, and 651° F.

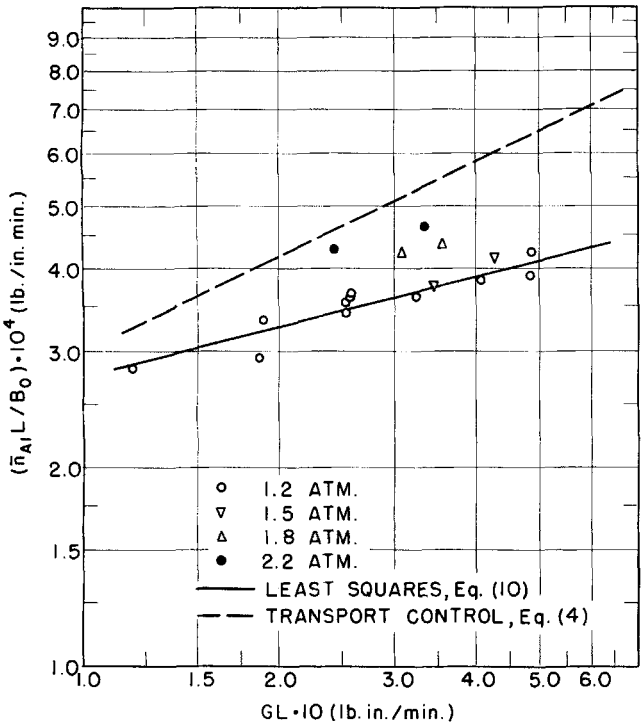

Fig. 3. Average rate data at 604° F.

with a slope of ½. On the other hand, for the rate controlled by surface reaction, the slope will, of course, be zero. Such a plot of the average rate data is shown in Figures 2 and 3. The data obtained at 505°F. scatter appreciably owing to the uncertainty in surface area; however, little effect of flow rate on reaction rate is noted. At other temperatures the data vary approximately as the ¼ power of N_{Re} and the 604°F. data indicate an effect of pressure not predicted by Equation (4). Thus over the range of variables that could be investigated the rate of reaction is neither chemically or transport controlled but lies in an intermediate regime.

The data in Figures 2 and 3 can be well correlated empirically at constant temperature and pressure by an equation of the form

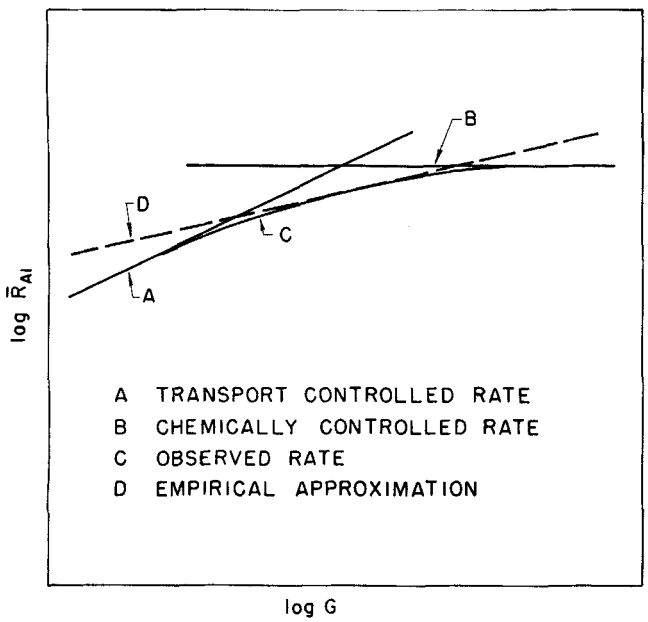

Fig. 4. Qualitative representation of theoretical dependence of reaction rate on flow rate.

Table 2. Calculation of Transport-Controlled Reaction Rates

Temperature, °F.	$\frac{\bar{n}_{Al}L}{B_o}$, lb./(in.)(min.)
505	$8.77 \times 10^{-3}\sqrt{GL}$
558	$8.99 \times 10^{-3}\sqrt{GL}$
604	$9.16 \times 10^{-3}\sqrt{GL}$
651	$9.35 \times 10^{-3}\sqrt{GL}$

G in pounds per minute; L in inches.

$$\frac{\bar{R}_{Al}\,L}{B_o} = a_1\ N_{Re}^{a_2} \tag{10}$$

but the dangers of extrapolating such an equation are shown in Figure 4.

For intermediate reactions several methods exist (*3, 4, 6, 7, 11*) for calculating the effect of mass transport on chemical reaction rates. The result obtained by Rosner (*11*) seems especially noteworthy since it combines accuracy with simplicity.

For systems with surface kinetics of the type

$$R_A = k_A\ (\rho\ \omega_{A,s})^n \tag{11}$$

and in which there is no net mass flux at the surface, Rosner gives the average reaction rate as

$$\bar{R}_A = k_A\ (\rho\ \omega_{A,e})^n \frac{2}{\omega_L{}^n} \left(\frac{1-\omega_L}{Z_L}\right)^2 \tag{12}$$

where

$$\omega = \omega_{A,s}/\omega_{A,e} \tag{13}$$

$$Z = \frac{k_A(\rho\omega_{A,e})^n}{N_{ShL}D\rho\omega_{A,e}/L} \left(\frac{x}{L}\right)^{1/2} \tag{14}$$

The unknown surface concentration (ω) and the distance parameter (Z) are related by

$$Z^2 = -\int_1^{\omega} \omega^{-(2n+1)}\ (1-\omega)\ \ [2n-2\ (n-2)\omega]\ d\omega \tag{15}$$

and ω_L is the value of ω evaluated at $Z = Z_L$ ($x = L$). Solution of these equations is difficult when n is to be determined from experimental data. However, above a certain value for Z_L, Equation (15) may be approximated by

$$Z_L^2 \cong \frac{1}{\omega_L^{2n}} \tag{16}$$

except for $n = 0$. Substitution of this approximation into Equation (12) leads to

$$\frac{\bar{R}_A}{\bar{n}_A} = \left(1-\frac{1}{Z_L{}^{1/n}}\right)^2 \tag{17}$$

where $\bar{n}_A$ is the transport-controlled reaction rate given by

$$\bar{n}_A = \frac{\rho_s D_A}{L}\omega_{A,e}\ \overline{N_{Sh}} \tag{18}$$

Replacing Z_L by its value given in Equation (14) and rearranging one gets

$$\frac{\bar{n}_A}{2\,k_A} = \left\{(\rho\ \omega_{A,e})\left[\ 1-\sqrt{\frac{\bar{R}_A}{\bar{n}_A}}\ \right]\right\}^n \tag{19}$$

When this equation is applied to the aluminum–chlorine

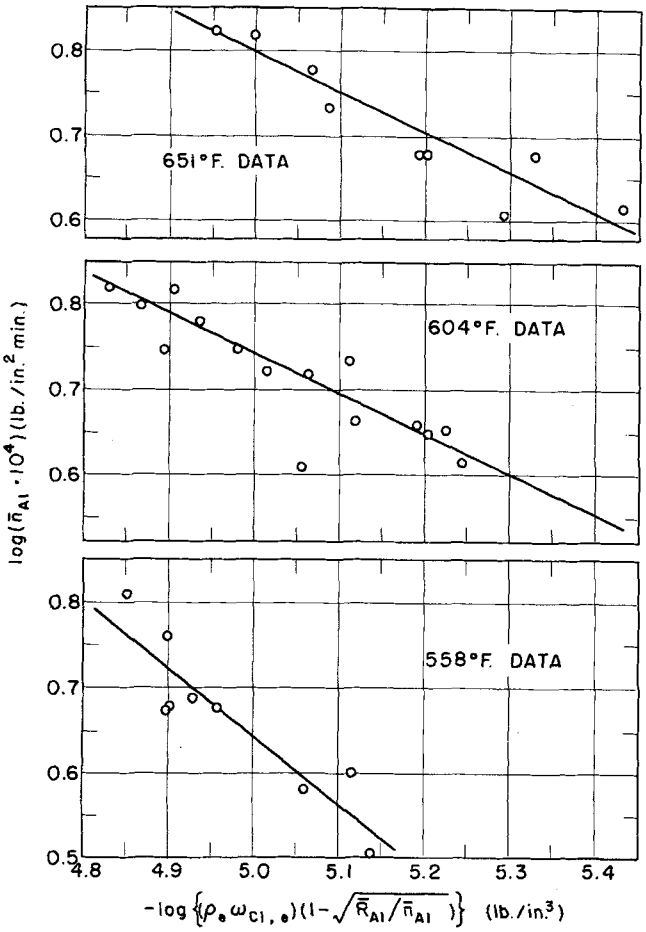

Fig. 5. Correlation of the data from Equation (19a).

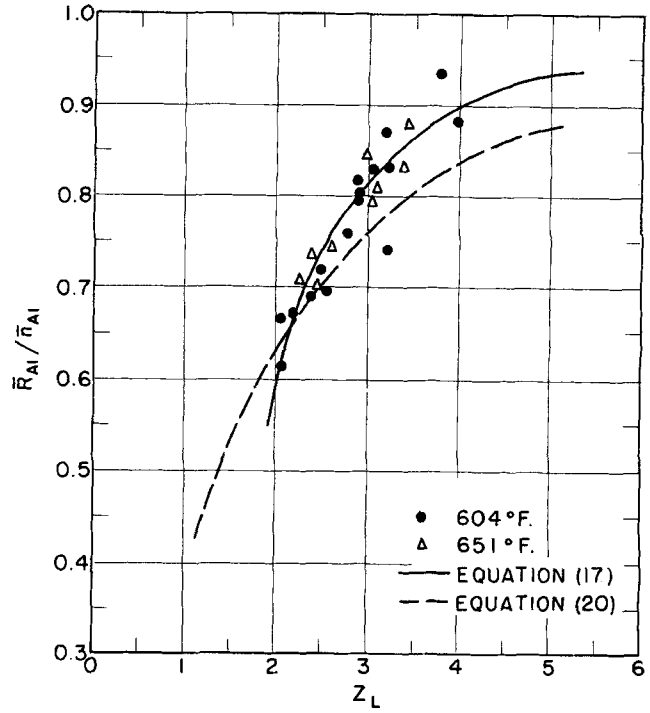

Fig. 6. Correlation of the average rate data for $n = 0.469$.

reaction, $\bar{R}_A$ and $\bar{n}_A$ denote the reactions rate of chlorine. Since the reaction rate of chlorine is related to that of aluminum by stoichiometry, Equation (19) can also be written as

$$\frac{\bar{n}_{Al}}{2\,k_{Al}} = \left\{(\rho\,\omega_{Cl,e})\left[1-\sqrt{\frac{\bar{R}_{Al}}{\bar{n}_{Al}}}\right]\right\}^n \qquad (19a)$$

and Equation (11) for the surface reaction rate as

$$R_{Al} = k_{Al}\,(\rho\,\omega_{Cl,s})^n \qquad (11a)$$

Equation (19a) is now in a form convenient for determining values of k_{Al} and n from the data obtained for a logarithmic plot of $\bar{n}_{Al}$ vs. the right-hand side of Equation (19a) gives a straight line with slope equal to n and intercept log $2k_{Al}$.

Equation (19) was derived for constant physical property systems with no net mass flux at the plate surface. Neither of these conditions was met in this study. The effect of the convective mass transport at the plate surface is small, however, and it was assumed that suitable values of $\bar{n}_{Al}$ could be calculated from Equations (18) and (7) by using average physical properties and by assuming ρ_s is given by the density of Al_2Cl_6.

Using the estimation procedures given by Bird et al. (*1*) for the calculation of molecular force constants, viscosity and mass diffusivity, and arbitrarily evaluates the Schmidt and Reynolds numbers at a chlorine mass fraction of 0.3, we calculated values of $\bar{n}_{Al}\,L/B_o$ as shown in Table 2. These equations are plotted in Figures 2 and 3.

With these values of $\bar{n}_{Al}L/B_o$ and experimental values of $\bar{R}_{Al}$, Equation (19a) is plotted in Figure 5 for the data at 558°, 604°, and 651°F. The data appear approximately linear and were correlated by least squares to determine the values of k_{Al} and n. The results of this correlation and the correlation coefficient r^2 are shown in Table 3.

The values of n obtained are in good agreement at 604° and 651°F., but these values appreciably differ from the value obtained at 558°F. Statistical comparison of the values of n gives 94% probability that the n's at 604° and 651°F. are the same. When one assumes that the re-

Table 3. Values of the Kinetic Parameters

Temperature, °F.	k_{Al}	n	r^2
558	2.215	0.801	0.823
604	0.0651	0.476	0.840
651	0.0634	0.462	0.889

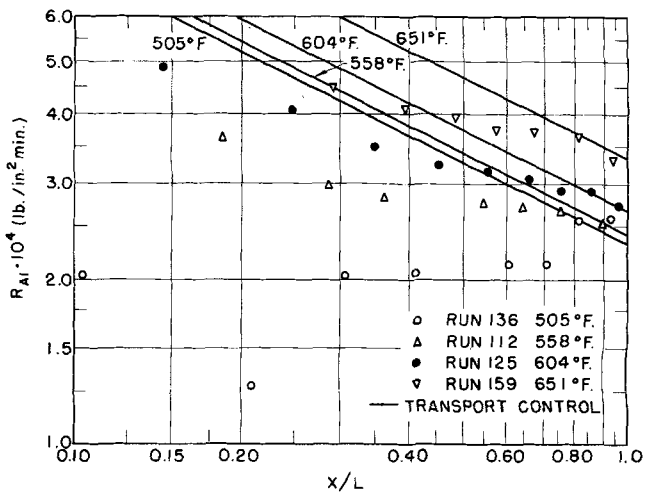

Fig. 7. Local rate data.

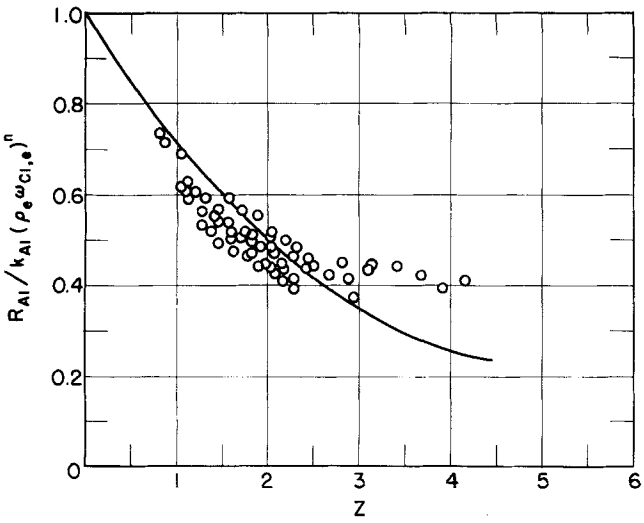

Fig. 8. Local rate data at 558°F.

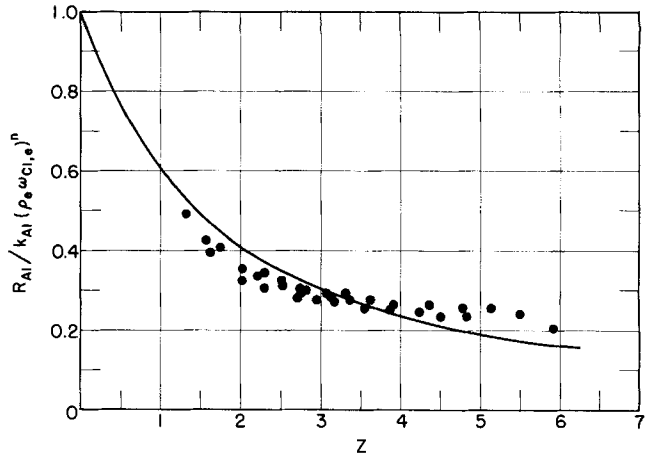

Fig. 9. Local rate data at 604° and 651°F.

action orders at 604° and 651°F. are actually equal and given by the average of the results, then n equals 0.469 and the rate constants are $k_{Al} = 0.0610$ at 604° and 0.0678 at 651°F.

It may now be of interest to compare the approximate solution given by Equation (17) with the exact solution by Equation (12). Written in terms of aluminum reaction rate, Equation (12) becomes

$$\frac{\overline{R}_{Al}}{n_{Al}} = \frac{1}{Z_L}\left[\frac{1}{\omega_L{}^n}(1-\omega_L)^2\right] \qquad (20)$$

This equation is compared with Equation (17) in Figure 6 for a value of n equal to 0.469. Also shown are the 604° and 651°F. data. Over the range of Z_L investigated, Equation (17) deviates from Equation (20) by a maximum of 7% and is a good approximation to the exact equation when Z_L is greater than 2. Similar results are obtained with the 558°F. data.

Local Rate Data

Local reaction rates were determined for several representative runs in each temperature series. These rates represent the reaction rates over ¼ in. segments of the aluminum specimens. Some typical data are shown plotted in Figure 7 as log R_{Al} vs. log (x/L) (the x coordinate for each piece was measured from the leading edge of the plate to the center of the piece). Also shown on this figure is the transport-controlled rate as calculated from the equation

$$n_{Al} = \frac{1}{2}\, n_{Al}\left(\frac{L}{x}\right)^{1/2} \qquad (21)$$

where $\overline{n}_{Al}$ is given by Equation (4).

The data at 505°F. show considerable scattering as would be expected since the samples pitted. However, there appears to be little effect of length on the reaction rate, again indicating chemical control at this temperature. The data at the other temperatures show an effect of length on reaction rates; however, the effect is less than for a transport-controlled reaction.

To correlate the local rate data Equations (11) and (15) were combined to eliminate the unknown surface concentration (ω), thus giving a relation between R_{Al} and Z. The measured local rates are compared with the calculated rates in Figures 8 and 9. Good agreement between the measured and predicted local rates is noted. Thus the local rate data generally confirm Rosner's equations and the kinetic parameters calculated from the average rate data.

CONCLUSIONS

The reaction between aluminum and chlorine at temperatures from 500° to 650°F. appears to undergo several changes in mechanism. At 500°F. the surface activity of the aluminum is not uniform, and the reaction takes place in localized areas of high activity leaving a pitted surface. Experiments with high purity aluminum indicate the highly active areas are at the grain boundaries. At higher temperatures uniform surface activity is obtained; however, the dependence of reaction rate on chlorine concentration changes between 550° and 600°F.

Owing to the assumptions contained in the correlating equations and the necessity of a priori postulating a surface reaction rate given by Equation (11), the true kinetics of this reaction has not been definitely established. However, for heterogeneous reactions of unknown kinetics in which mass transport affects the reaction rate, the equations proposed by Rosner appear to present the best method of correlating both average and local reaction rates.

ACKNOWLEDGMENT

This work was supported in part by the Allied Chemical Company and the American Oil Company. The authors are also grateful to the Alcoa Research Laboratories for their assistance.

NOTATION

A = surface area, sq.in.
a, b, c, a_1, a_2 = constants
B = mass transfer parameter defined by Equation (5), dimensionless
D = mass diffusivity, sq.in./min.
G = mass flow rate of chlorine, lb./min.
k = kinetic rate constant
k_D = mass transfer coefficient
L = plate length, in.
M = molecular weight
n = reaction order
n_A = local mass flux or local transport controlled reaction rate of component A, lb./(sq.in.)(min.)
N_{Re} = Reynolds number, $LU\rho/\mu$
N_{Sh} = local Sherwood number, $k_D L/D$
R_A = local reaction rate of component A, lb./(sq.in.)(min.)

U = velocity outside the boundary layer, in./min.
W = aluminum plate weight, lb.
x = coordinate parallel to the plate surface
Z = variable defined by Equation (14), dimensionless

Greek Letters

α = constant defined by Equation (6)
θ = time, min.
μ = viscosity
ρ = mass density, lb./cu.in.
ω = mass fraction, dimensionless

Subscripts

A, B, C = component, A, B, C,
e = evaluation outside the boundary layer
L = evaluation at $x = L$
s = evaluation at the plate surface

Superscripts

i = initial
f = final
$\overline{\ }$ = average

LITERATURE CITED

1. Bird, R. B., W. E. Stewart, and E. N. Lightfoot, "Transport Phenomena," pp. 22, 511, 746, Wiley, New York (1960)
2. Brown, M. H., W. B. DeLong, and J. P. Auld, *Ind. Eng. Chem.*, **39**, 839 (1947).
3. Chambré, P. L., and Andreas Acrivos, *J. Appl. Phys.*, **27**, 1322 (1956).
4. Chung, P. M. and A. D. Anderson, *ARS J.*, **30**, 262 (1960).
5. Evans, M. *Manchester Mem.*, **79**, No. 2,13 (1934).
6. Frank-Kamenetskii, D. A., "Diffusion and Heat Exchange in Chemical Kinetics," p. 46, Princeton Univ. Press, N. J. (1955).
7. Levich, V. G., "Physiochemical Hydrodynamics," p. 93, Prentice-Hall, Englewood Cliffs, N. J. (1962).
8. Merk, H. J., *Appl. Sci. Res.* **A8**, 237 (1959).
9. *Ibid.*, 261.
10. Mickley, H. S., R. C. Ross, A. L. Squyers, and W. E. Stewart, *Natl. Advisory Comm. Aeronaut. Tech. Note 3208* (1954).
11. Rosner, D. E., *AIChE J.*, **9**, 321 (1963).
12. Spalding, D. B., *Proc. Roy. Soc. (London)*, **A221**, 78 (1954).

Manuscript received September 24, 1965; revision received December 5, 1966; paper accepted December 5, 1966.

Sorption and Diffusion of Gaseous Hydrocarbons in Synthetic Mordenite

CHARLES N. SATTERFIELD and ALTON J. FRABETTI, JR.

Massachusetts Institute of Technology, Cambridge, Massachusetts

Diffusion coefficients for the C_1 to C_4 paraffin hydrocarbon gases in single crystals of the synthetic zeolite (molecular sieve) sodium mordenite were determined from transient sorption rate and desorption rate measurements over the temperature range 25° to 140°C. and pressure range 0 to 20 cm. Hg, and found to be of the order of 10^{-9} to 10^{-10} sq. cm./sec. Diffusion coefficients for desorption were from three to sixty times smaller than those for sorption. Activation energies for methane and ethane were 1.7 and 1.9 kcal./mole, respectively.

Equilibrium sorption capacity and diffusion coefficients are markedly affected by the conditions of synthesis and by mechanical treatments such as grinding. For propane at 29°C. and at 2.0 cm. Hg pressure, the sorption capacity in 2.5 μ crystals was only 50% of that in 21 by 21 by 33 μ crystals and the diffusion coefficient was only 1/50 of that in the larger crystals. Light mechanical grinding of the larger crystals lowered the sorption capacity 30% and the diffusion coefficient by a factor of 35.

Mordenite is a zeolite (molecular sieve) having the ideal formula (hydrated) in the sodium form of $Na_2O(Al_2O_3)(SiO_2)_{10}\cdot 6H_2O$. By varying the synthesis conditions, the atomic ratio of silicon to aluminum can be varied from about 4½ to 5½ without essentially altering the crystal structure, although the cation density will change. Mordenite is one of the few zeolites that will undergo complete hydrogen ion exchange in moderately acidic media without destruction of the crystal structure. The structures of zeolites in general are described, for example, in the book by Hirsch (*22*) and the review of Breck (*17*). They all consist of a three-dimensional framework of SiO_4 and AlO_4 tetrahedra, which can be arranged in a variety of ways. The crystal structure of mordenite was reported by Meier in 1961 (*23*) to be such that the principal sorption channels are formed by twelve-membered rings of silica-alumina tetrahedra, the passageways being elliptical in shape with major and minor diameters of 7.0 and 5.8 Å. However, the sorption characteristics of mordenite as reported during the period 1948-1954 by Barrer and co-workers (*4* to *6*, *12* to *14*) on material synthesized in his laboratory are consistent only with passageways with restrictions of the order of 4 Å. in diameter, so Meier suggested that stacking faults existed in Barrer's mordenite. But, stacking faults seem to imply considerable strain and a more plausible explanation is that the pores of this and other zeolites may be partly obstructed in various places by cations or by other substances. The

Alton J. Frabetti, Jr., is at General Electric Company, Pittsfield, Massachusetts.